



# Intermolecular interactions between the SH3 domain and the proline-rich TH region of Bruton's tyrosine kinase

Henrik Hansson<sup>a</sup>, Mishael P. Okoh<sup>b,s</sup>, C.I. Edvard Smith<sup>d,e</sup>, Mauno Vihinen<sup>s,f</sup>,  
Torleif Hård<sup>a,\*</sup>

<sup>a</sup>Department of Biotechnology, Royal Institute of Technology (KTH), Centennial Laboratory of Biochemistry, Notum, S-141 57 Huddinge, Sweden

<sup>b</sup>Institute of Medical Technology, University of Tampere, P.O. Box 607, FIN-33101 Tampere, Finland

<sup>s</sup>Department of Biocenter, Division of Biochemistry, University of Helsinki, P.O. Box 56, FIN-00014 Helsinki, Finland

<sup>d</sup>Department of Biocenter at Notum, Kavolinranta Institute, S-141 57 Huddinge, Sweden

<sup>e</sup>Clinical Research Centre, Kavolinranta Institute, Huddinge University Hospital, S-141 86 Huddinge, Sweden

<sup>f</sup>Tampere University Hospital, FIN-33520 Tampere, Finland

Received 23 November 2000; accepted 19 December 2000

First published online 11 January 2001

Edited by Gianni Cesareni

**Abstract** The SH3 domain of Bruton's tyrosine kinase (Btk) is preceded by the Tes homology (TH) region containing proline-rich sequences. We have studied a protein fragment containing both the Btk SH3 domain and the proline-rich sequences of the TH region (PRR-SH3). Intermolecular NMR cross-relaxation measurements, gel permeation chromatography profiles, titrations with proline-rich peptides, and <sup>15</sup>N NMR relaxation measurements are all consistent with a monomer-dimer equilibrium with a dissociation constant on the order of 60 μM. The intermolecular interactions do, at least in part, involve proline-rich sequences in the TH region. This behavior of Btk PRR-SH3 may have implications for the functional action of Btk. © 2001 Federation of European Biochemical Societies. Published by Elsevier Science B.V. All rights reserved.

**Key words:** Bruton's tyrosine kinase; Tes homology 3; Dimerization; Nuclear magnetic resonance; Gel permeation chromatography; Signal transduction

## 1. Introduction

Mutations in the gene encoding Bruton's tyrosine kinase (Btk) cause the hereditary immunodeficiency X-linked agammaglobulinemia (XLA) [1,2]. Btk belongs to the Tes-family of non-receptor (cytoplasmic) tyrosine kinases [3]. XLA-causing mutations have been found in all five subdomains of Btk [4]. Tes homology 3 (SH3) domains interact with proline-rich motifs with the consensus sequence PXXP [5–7] and this is also the case for the SH3 domain of Btk [8].

Activation of Btk occurs through phosphorylation of a tyrosine in the activation loop of the kinase domain [9] followed by an autophosphorylation of Y223 within the SH3 domain

[10]. Self-regulation of kinase activity through interaction involving SH3 domains has been reported for Src-family kinases Src and Hsk [11,12]. The Tes homology (TH) region of Btk, located N-terminal to the SH3 domain, contains two PXXP motifs, whereas the closely related kinases Itk and Bmx contain only one. For Itk it was shown [13] that the PXXP motif of the TH region binds intramolecularly to the SH3 domain in a possible self-regulating manner. Here we study an N-terminally extended fragment of Btk SH3 containing the proline-rich sequences of the TH region: the PRR-SH3 fragment. We find that, in contrast to the situation in Itk, the Btk SH3 domain interacts with the TH region in an intermolecular manner. This self-association of PRR-SH3 fragments, most likely in the form of a homodimer, involves binding of a PXXP motif to the binding pocket of the SH3 domain. We suggest that the interaction has implications for the activation of Btk.

## 2. Materials and methods

### Cloning, expression and purification

The cloning, expression and purification of the Btk SH3 domain have been reported earlier [14]. For the N-terminally extended SH3 (PRR-SH3), the DNA fragment encoding residues 178–275 of human Btk was amplified by PCR and the fragment was cloned into the pGEX-4T-3 vector (Amersham Pharmacia Biotech, Sweden) for expression in *Escherichia coli* BL21 (DE3). The expression and purification of unlabeled, <sup>15</sup>N-labeled, and <sup>13</sup>C,<sup>15</sup>N-labeled Btk PRR-SH3 and SH3 for the present study was essentially carried out as reported previously [14]. In addition, purified protein samples were heat-stabilized in Eppendorf tubes at 65°C for 30 min immediately followed by cooling to 4°C and centrifugation at 21 000Xg for 10 min. This procedure effectively inactivated and removed contaminant proteins. The mass of PRR-SH3 was confirmed using MALDI-TOF mass spectrometry. The protein concentration was measured by absorbance at 278 nm using an extinction coefficient of 18 000 M<sup>-1</sup> cm<sup>-1</sup>.

### Analytical gel permeation chromatography (GPC)

A Superdex 75 HR 10/30 (Amersham Pharmacia Biotech) column attached to an ALTA purifier system, was equilibrated with several column volumes of phosphate buffer. For each run, 0.1 ml of protein sample was applied to the column. The elution was performed at 0.5 ml min<sup>-1</sup> and protein absorbance was detected at 280 nm. The retention behavior was characterized by an average partition coefficient  $\alpha_{av} = (V_e - V_M)/V_s$ , where  $V_e$  is the elution volume corresponding to the maximum of the elution profile,  $V_M$  is the void volume of the mobile phase and  $V_s$  is the volume available to a totally included solute. The suitability of the selected column for separation in a mo-

\*Corresponding author. Fax: (46)-8-6089290.  
E-mail: torleif.hard@bioshem.kth.se

Abbreviations: Btk, Bruton's tyrosine kinase; SH3 domain, Tes homology 3 domain; TH region, Tes homology region; PRR-SH3, N-terminally extended Btk SH3 domain containing the proline-rich sequences of the TH region; NMR, nuclear magnetic resonance; GPC, gel permeation chromatography

lesular weight range covering monomer and dimer of PRR-SH3 was confirmed by the elution profile of a Gel Filtration-Low Molecular Weight Calibration kit standard (Amersham Pharmacia Biotech).

The non-linear retention behavior of PRR-SH3 at various concentrations was modeled using the Craig method of propagating the injected volume through a grid of theoretical plates [15]. The retention at each plate along the grid was calculated from the effective concentration-dependent partition coefficient for a monomer-dimer equilibrium given by  $o_{eff} = o_2 + a(o_1 - o_2)$ , where  $o_1$  and  $o_2$  represent partition coefficients for monomer and dimer of PRR-SH3, respectively. The fraction of monomers is given by  $a = K_d [-1 + (8c_0/K_d + 1)^{1/2}] / 4c_0$ , where  $c_0$  is the total PRR-SH3 concentration (which decreases as the sample is propagated down the column), and  $K_d$  is the dissociation constant for the dimerization equilibrium. The unknown parameters  $o_1$ ,  $o_2$ , and  $K_d$  were estimated by fitting  $o_{av}$  as a function of loaded concentrations using unstrained non-linear least-squares optimization. The number of plates assumed in the fit and the simulation were 900, as this value best reproduced the observed elution profiles.

#### Nuclear magnetic resonance (NMR) spectroscopy

NMR was measured at 30 and 45°C using Varian Inova 500, Bruker DRX 500 and DRX 600 spectrometers equipped with 5 mm

triple-resonance ( $^1H/^{15}N/^{13}C$ ) probes. Two-dimensional  $^1H$ - $^{15}N$  HSQC and three-dimensional NOESY-HSQC experiments were carried out and processed using conventional methods [16]. Intermolecular cross-relaxation was detected in two-dimensional  $F_1$ - $^{13}C$ -edited,  $F_2$ - $^{13}C$ ,  $^{15}N$ -filtered NOESY experiments (following the principles described in [17]) recorded at 45°C on a sample containing a mixture of unlabeled and doubly labeled PRR-SH3 at a total concentration of

2.5 mM. The  $^{13}C$  transmitter offset and refocusing delays for the pulse scheme were set to optimize purging of either aliphatic or aromatic  $^{13}C$ -bound proton resonances. The cross-relaxation mixing time in these experiments was 100 ms.

#### Peptide titration

Peptides corresponding to residues 181–192 of the TH region of Btk with an additional tyrosine and glutamine residue at the C-terminus (HRLTLLPLPPTYQ) were purchased from Ansynth Service B.V. (Roosendaal, The Netherlands). The peptide used for titration to Btk SH3 contained a C-terminal amidation which the peptide used for titration to Btk PRR-SH3 did not contain. The same peptide sequence was used in a peptide binding study on Btk SH3 [8]. The peptides were dissolved in phosphate buffer at pH 6.5 and their concentrations were measured by absorbance at 275 nm using the molar extinction coefficient of tyrosine ( $1420 M^{-1} cm^{-1}$ ). Samples containing 0.6 ml of

0.4 mM  $^{15}N$ -labeled SH3 or PRR-SH3 were prepared in NMR-tubes and the titrations were performed by adding peptide to the tube and recording an HSQC spectrum after each addition.

#### NMR relaxation measurement

Longitudinal and transverse relaxation rates,  $R_1$  and  $R_2$ , of backbone  $^{15}N$  nuclei in well structured regions of the SH3 domain were measured as reported previously [14]. The overall rotation correlation time,  $\tau_s$ , was estimated from  $\tau_s = 1 / \omega_0 (2(R_2/R_1))^{1/2}$  where  $\omega_0$  is the  $^{15}N$  Larmor frequency and the  $(R_2/R_1)$  average was measured for residues in stable secondary structure elements within the SH3 domain [16].

### 3. Results

#### GPC

In order to investigate the role of SH3 binding sequences present in the TH region of Btk we first analyzed the behavior of the two protein fragments in GPC. The retention of Btk PRR-SH3 on the GPC column is clearly concentration dependent while that of the Btk SH3 is independent of concentration (Fig. 1). In addition, the elution profiles of PRR-SH3 show clear trailing, whereas those of SH3 (and of other controls) are symmetric. The trailing signifies the non-linear retention behavior expected for concentration-dependent self-association. The peak retention data are consistent with a

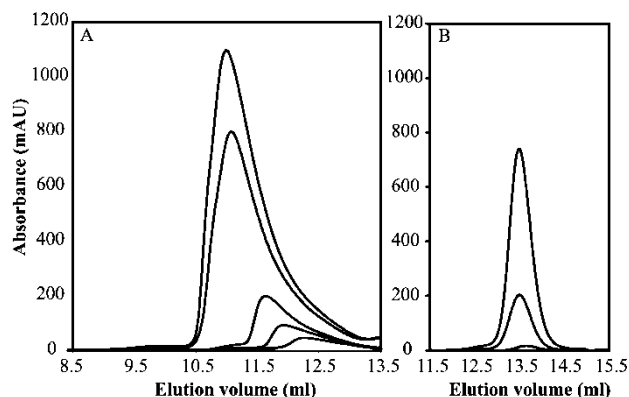


Fig. 1. GPC elution profiles. A: Btk PRR-SH3 applied at 1.1 mM, 0.8 mM, 0.2 mM, 0.1 mM and 0.05 mM. B: Btk SH3 applied at 0.57, 0.14 and 0.02 mM.

monomer-dimer equilibrium with a dissociation constant  $K_d = 6 \times 10^{-5} M$ , as shown in Fig. 2. Simulations also nicely reproduce the observed asymmetric elution profiles for PRR-SH3 (not shown).

#### The NMR spectrum of PRR-SH3 and its concentration dependence

The difference in NMR chemical shifts between PRR-SH3 and SH3 was analyzed. Sidechain resonances of Y223, M226, W251, W252, S247, I264 and N267 are among those that have large chemical shift differences. The backbone resonances of M228 and N229 in the RT-loop and E245 and S247 in the n-Srs loop are affected, as are those of Y225, W251, W252, R253, I264, S266, N267 and Y268. These are all within or close to the proposed poly-proline binding pocket on SH3. There are also unassigned NOEs involving the structured SH3 part of PRR-SH3, which are not present in SH3 (not shown).

A comparison of the HSQC spectrum of PRR-SH3 recorded at different protein concentrations (Fig. 3) with an HSQC spectrum of SH3 reveals that the differences in backbone chemical shifts between PRR-SH3 and SH3 decrease with the protein concentration. As seen in Fig. 3, the chemical shift differences for I264 and N267 are significant at 2 mM, but small at 0.02 mM. The same is true for nearly all of the residues that display different chemical shifts in PRR-SH3 as compared to the isolated SH3 (not shown) with D232 as the only exception. The dilution of PRR-SH3 is associated with sharpening of most backbone amide resonances. The concentration dependence and linewidths as a function of concentration are consistent with a monomeric state of PRR-SH3 at low concentrations and a dimeric state at higher concentrations.

To prove the existence of intermolecular interactions at higher concentrations we performed cross-relaxation experiments on a mixture of isotopically labeled and unlabeled PRR-SH3 at a 2.5 mM total concentration. The experiments were designed to excite  $^{13}C$ -bound protons and detect only  $^{12}C$  or  $^{14}N$ -bound protons. Cross-relaxation (NOEs) can in this case only be observed in structured aggregates (dimers) of labeled and unlabeled protein fragments. Several NOEs were detected in these experiments, as illustrated in Fig. 4, which shows intermolecular NOEs between aliphatic and aromatic proton resonances.

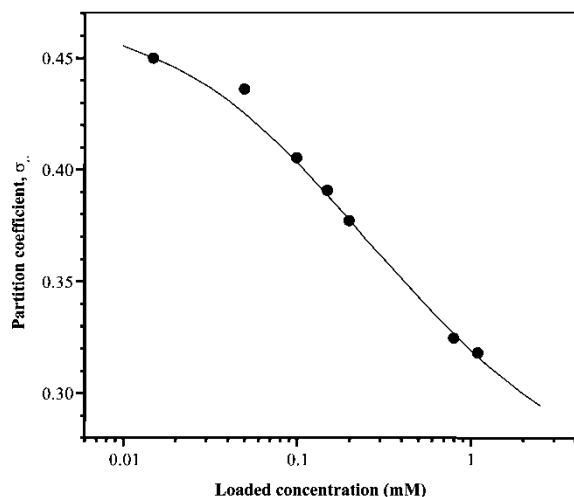


Fig. 2. Quantitative analysis of the concentration dependence of Btk PRR-SH3 elution from the GPC column. The observed average partition coefficient,  $\sigma_{av}$ , is plotted as function of the concentration of the applied sample. The solid line represents a fit of the data to a monomer–dimer equilibrium model with a dissociation constant  $K_d$  of 60  $\mu\text{M}$ .

Introduction of a TH3 binding sequence from the TH region as a peptide

To investigate if peptide binding could shift the equilibrium towards monomeric PRR-SH3 we titrated a TH-peptide (see Section 2) onto a  $^{15}\text{N}$ -labeled sample and monitored changes in the NMR spectrum. The amide backbone resonances of Y225, W251, W252, I264 and N267 are significantly narrower at 0.25 mM PRR-SH3 with excess TH-peptide compared to

0.3 mM without peptide. In addition, peptide binding has approximately the same effect on the PRR-SH3 spectrum as its concentration increases (Fig. 3). These observations are consistent with breaking a dimer by excess peptide, but introducing a chemical environment for the involved resonances which is similar to a fully dimerized sample. In other words, they link the dimer association behavior of PRR-SH3 to the TH region. In a control experiment we added TH-peptide to SH3 and observed the same chemical shift changes upon peptide binding to isolated SH3, as expected.

#### Rotation correlation time

In a final set of experiments we used  $^{15}\text{N}$  relaxation data to estimate the rotation correlation time,  $\tau_s$ , for Btk PRR-SH3

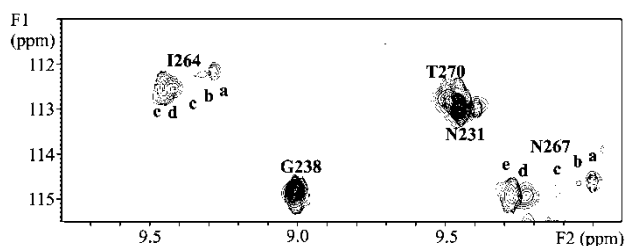


Fig. 3. Section of the  $^{15}\text{N}$  HSQC NMR spectrum of Btk PRR-SH3 and Btk SH3 samples. Backbone amide assignments have been indicated. The resonances of I264 and N267 under different conditions are annotated as follows: a: Btk SH3 reference; b–d: Btk PRR-SH3 at 0.02, 0.3 and 2 mM concentrations, respectively, and e: 0.25 mM PRR-SH3 with 5 mM TH-peptide.

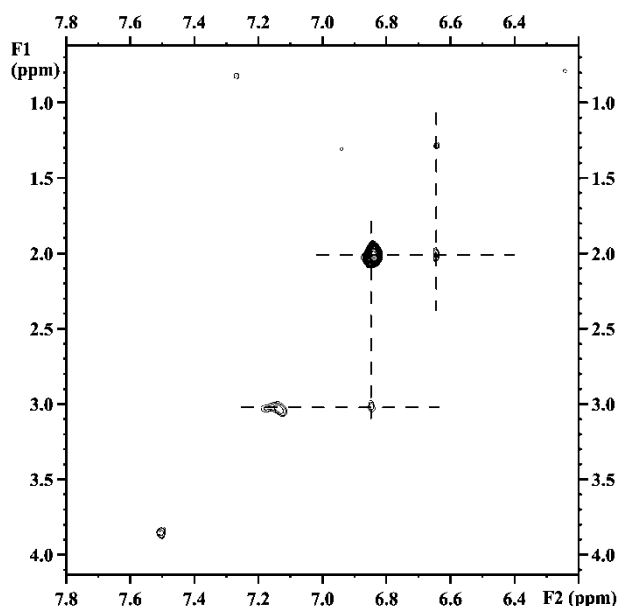


Fig. 4. Section of a  $F_1$ - $^{13}\text{C}$ -edited,  $F_2$ - $^{13}\text{C}$ ,  $^{15}\text{N}$ -filtered NOESY experiment resorted on a mixture of unlabeled and doubly labeled PRR-SH3 at a total concentration of 2.5 mM. The experiment was optimized for editing of  $^{13}\text{C}$ -bound aliphatic protons in  $F_1$  and filtering of  $^{13}\text{C}$ -bound aromatic and  $^{15}\text{N}$ -bound proton resonances in  $F_2$ . The dashed lines connect NOEs with identical chemical shifts in  $F_1$  or  $F_2$ .

to 11 ns (at 2 mM). A comparison with the value previously reported for monomeric Btk SH3 (5.5 ns) again supports a monomer–dimer equilibrium in PRR-SH3 samples.

#### 4. Discussion

Self-regulation of non-receptor kinases through intramolecular interactions has been reported for several kinases [11,12,18,19]. For the SH3 domain of the Tec-family kinase Itk it has been shown that a SH3 binding sequence in an N-terminal extension binds in an intramolecular fashion to the binding pocket of the SH3 domain [13]. Here we find that this is not the case for Btk SH3. Instead, GPC elution profiles, intermolecular NMR cross-relaxation and  $^{15}\text{N}$  NMR relaxation measurements are consistent with a monomer–dimer equilibrium with a dissociation constant on the order of 60  $\mu\text{M}$ . In addition, comparison of chemical shifts and resonance linewidths as a function of concentration with those observed in TH-peptide titrations indicate that peptide binding competes with dimerization. Based on these results we conclude that the interaction between the TH region and the SH3 domain is intermolecular rather than intramolecular in protein fragments containing both the TH region and SH3 domain of Btk.

It has been shown that the autophosphorylation of Y223 within the SH3 domain regulates the kinase activity in vivo [13]. In in vitro experiments, active full-length Btk is able to phosphorylate recombinant Btk SH3 domain at Y223. Thus, full-length Btk can interact with its own SH3 domain through protein–protein interactions. Our experiments suggest how this interaction may occur. Dimerization of receptor tyrosine kinases and activation through trans-phosphorylation of tyrosines is known for some growth factor receptors e.g. the plate-

let-derived growth factor receptor [20]. Also, dimerization via SH3 domains has been reported for the p85 $\alpha$  regulatory subunit of phosphatidylinositol-3 kinase [21]. The observed self-association of PRR-SH3 opens up for the possibility that the autophosphorylation event in activation of Btk occurs rather than in *in vivo*. Another possibility is that the phosphorylation destabilizes a pre-formed Btk dimer. Both these scenarios may have implications for the understanding of Btk activation.

**Acknowledgement:** This work was supported by the Swedish Natural Sciences Research Council (NFR), the Swedish Foundation for Strategic Research (SSF), the Swedish Cancer Foundation and the European Union Grant BI04-CT98-0142.

#### References

- [1] Vetric, D., Voreshovsky, I., Sideras, P., Holland, J., Davies, A., Flinter, F., Hammarström, L., Linnon, C., Levinsky, R., Brown, M., Smith, C.I.E. and Bentley, D.R. (1993) *Nature* 361, 226–233.
- [2] Tsukada, S., SaRran, D.C., Rawlings, D.J., Parolini, O., Allen, R.C., Lisak, I., Sparkes, R.S., Lubagawa, H., Mohandas, T., Quan, S., Belmont, J.W., Cooper, M.D., Conley, M.E. and Witte, O.N. (1993) *Cell* 72, 279–290.
- [3] Smith, C.I.E., Islam, T.C., Mattsson, P.T., Mohamed, A.J., Nore, B.F. and Vihinen, M. (2000) *Bioessays*, in press.
- [4] Vihinen, M., Lwan, S.-P., Lester, T., Oshs, H.D., Resnisk, I., Väliäho, J., Conley, M.E. and Smith, C.I.E. (1999) *Hum. Mutat.* 13, 280–285.
- [5] Saha, B.L., Curtis, S.L., Vogler, L.B. and Vihinen, M. (1997) *Mol. Med.* 3, 477–485.
- [6] Ren, R., Mayer, B.J., Cisschetti, P. and Baltimore, D. (1993) *Science* 259, 1157–1161.
- [7] Yu, H., Chen, J.L., Feng, S., Dalgarno, D.C., Brauer, A.W. and Sshreiber, S.L. (1994) *Cell* 76, 933–945.
- [8] Patel, H.V., Tzeng, S.R., Liao, C.Y., Chen, S.H. and Cheng, J.W. (1997) *Proteins* 29, 545–552.
- [9] Rawlings, D.J., Ssharenberg, A.M., Park, H., Wahl, M.I., Lin, S., Lato, R.M., Fluskiger, A.-C., Witte, O.N. and Linet, J.-P. (1996) *Science* 271, 822–825.
- [10] Park, H., Wahl, M.I., Afar, D.E.H., Turck, C.W., Rawlings, D.J., Tam, C., Ssharenberg, A.M., Linet, J.-P. and Witte, O.N. (1996) *Immunity* 4, 515–525.
- [11] Xu, W., Harrison, S.C. and Esk, M.J. (1997) *Nature* 385, 595–602.
- [12] Sisheri, F., Moarefi, I. and Luriyan, J. (1997) *Nature* 385, 602–609.
- [13] Andreotti, A.H., Bunnell, S.C., Feng, S., Berg, L.J. and Sshreiber, S.L. (1997) *Nature* 385, 93–97.
- [14] Hansson, H., Mattsson, P.T., Allard, P., Haapaniemi, P., Vihinen, M., Smith, C.I.E. and Hard, T. (1998) *Biochemistry* 37, 2912–2924.
- [15] Czok, M. and Guishon, G. (1990) *Anal. Chem.* 62, 189–200.
- [16] Cavanagh, J., Fairbrother, W.J., Palmer, A.G. and Skelton, N.J. (1996) *Protein NMR Spectroscopy: Principles and Practice*, Academic Press, London.
- [17] Vuister, G.W., Lim, S.-J., Wu, C. and Bax, A. (1994) *J. Am. Chem. Soc.* 116, 9206–9210.
- [18] Nam, H.J., Haser, W.G., Roberts, T.M. and Frederisk, C.A. (1996) *Structure* 4, 1105–1114.
- [19] Moarefi, I., LaFevre-Bernt, M., Sisheri, F., Huse, M., Lee, C.-H., Luriyan, J. and Miller, W.T. (1997) *Nature* 385, 650–653.
- [20] Sshlessinger, J. (2000) *Cell* 103, 211–225.
- [21] Harpur, A.G., Layton, M.J., Das, P., Bottomley, M.J., Panayotou, G., Drissoll, P.C. and Waterfield, M.D. (1999) *J. Biol. Chem.* 274, 12323–12332.